

# Vortex solitons of the discrete Ginzburg-Landau Equation

C. Mejía-Cortés and J.M. Soto-Crespo  
*Instituto de Óptica, C.S.I.C., Serrano 121, 28006 Madrid, Spain*

Rodrigo A. Vicencio and Mario I. Molina

*Departamento de Física, Facultad de Ciencias, Universidad de Chile, Casilla 653, Santiago, Chile and  
 Center for Optics and Photonics, Universidad de Concepción, Casilla 4016, Concepción, Chile*

(Dated: November 2, 2018)

We have found several families of vortex soliton solutions in two-dimensional discrete dissipative systems governed by the cubic-quintic complex Ginzburg-Landau equation. There are symmetric and asymmetric solutions, and some of them have simultaneously two different topological charges. Their regions of existence and stability are determined. Additionally, we have analyzed the relationship between dissipation and stability for a number of solutions. We have obtained that dissipation favours the stability of the solutions.

PACS numbers: 42.65.Wi, 63.20.Pw, 63.20.Ry, 05.45.Yv

## I. INTRODUCTION

An optical vortex soliton is a self localized nonlinear wave, characterized for having a point ('singularity') of zero intensity, and with a phase that twists around that point, with a total phase accumulation of  $2\pi S$  for a closed circuit around the singularity [1]. The quantity  $S$  is an integer number known as the vorticity or topological charge of the solution. Optical vortices can exist in an infinite number of ways, as there is no limit to the topological charge. This kind of waves looks attractive in future applications for encoding and storing information. A spatial vortex soliton is a specific solution for a (2+1) dimensional nonlinear wave equation [2]. One of the most widely used equations of such a type is the nonlinear Schrödinger equation (NLSE); it describes wave evolution in dispersive/diffractive continuous media with an optical Kerr response, i.e. a refractive index that changes linearly with the light intensity. When the system under consideration has a periodic structure, e.g. a photonic crystal fiber, it is necessary to add a periodic transversal potential to complete the description, in the NLSE. The optical properties of a nonlinear periodic structure can be analyzed in the framework of a set of linearly coupled-mode equations which, in solid-state physics is called the *tight-binding* approximation, so that the description of the system can be understood from a discrete point of view. The study of discrete systems has been a hot topic in the last years due both to its broad impact in diverse branches of science and its potential for technological applications [3–6]. Nonlinear optical systems allow us to observe several self-localized discrete structures in both spatial and temporal domains.

Unlike conservative systems, self-localized structures in systems far from equilibrium, are dynamical solutions that exchange energy with an external source (open systems). These solutions are called dissipative solitons [7]. In Schrödinger models, gain and loss are completely neglected and the dynamical equilibrium is reached by means of a balance between the Kerr effect and dis-

persion/diffraction. For dissipative systems, there must also exist an additional balance between gain and losses, turning the equilibrium into a many-sided process [8]. The Ginzburg-Landau equation is -somehow- a universal model where dissipative solitons are their most interesting solutions. This model appears in many branches of science like, for example, nonlinear optics, Bose-Einstein condensates, chemical reactions, super-conductivity and many others [9].

Nonlinear self-localized structures in optical lattices, usually referred to as discrete solitons, have been predicted and observed for one- and two-dimensional arrays [10, 11]. The existence of discrete vortex solitons in conservative systems have been reported on several works [12–14]. For the continuous case, dissipative vortex soliton families have been found to be stable for a wide interval of  $S$ -values [15, 16]. Symmetric stable vortices have also been predicted in continuous dissipative systems with a periodic linear modulation [17]. In this work, we deal with discrete vortex solitons in dissipative 2D lattices governed by a discrete version of the Ginzburg-Landau equation. We have found different families of these self-localized solutions. We studied their stability and found stable vortex families for  $S = 3$  (symmetric) and  $S = 2$  (asymmetric) topological charges for the same set of equation parameters. In addition, we found another symmetric solution in which two topological charges ( $S = 2$  and  $S = 6$ ) coexist. Finally, we show how an increase in dissipation increases the stability regions for the same "swirl-vortex" soliton analyzed in the recent work [18].

The paper is organized as follows. In Section II we portray the model that we are going to use in the rest of the paper. Sections III and IV describe the new families of solutions we obtain, and in Section V we compare the results of our dissipative model with the conservative cubic case (Schrödinger limit). Finally, section VI summarizes our main results and conclusions.

## II. MODEL

### A. The cubic quintic Ginzburg-Landau equation

Beam propagation in 2D dissipative waveguide lattices can be modeled by the following equation:

$$i\dot{\psi}_{m,n} + \hat{C}\psi_{m,n} + |\psi_{m,n}|^2\psi_{m,n} + \nu|\psi_{m,n}|^4\psi_{m,n} = i\delta\psi_{m,n} + i\varepsilon|\psi_{m,n}|^2\psi_{m,n} + i\mu|\psi_{m,n}|^4\psi_{m,n}. \quad (1)$$

Eq.(1) represents a physical model for open systems that exchange energy with external sources and it is called (2+1)*D* discrete complex cubic-quintic Ginzburg-Landau (CQGL) equation.  $\psi_{m,n}$  is the complex field amplitude at the  $(m, n)$  lattice site and  $\dot{\psi}_{m,n}$  denotes its first derivative with respect to the propagation coordinate  $z$ . The set

$$\{m = -M, \dots, M\} \times \{n = -N, \dots, N\},$$

defines the array,  $2M + 1$  and  $2N + 1$  being the number of sites in the horizontal and vertical directions (in all our simulations  $M = N = 8$ ). The *tight binding* approximation establishes that the fields propagating in each waveguide interact linearly only with nearest-neighbor fields through their evanescent tails. This interaction is described by the discrete diffraction operator

$$\hat{C}\psi_{m,n} = C(\psi_{m+1,n} + \psi_{m-1,n} + \psi_{m,n+1} + \psi_{m,n-1}),$$

where  $C$  is a complex parameter. Its real part indicates the strength of the coupling between adjacent sites and its imaginary part denotes the gain or loss originated by this coupling. The nonlinear higher order Kerr term is represented by  $\nu$  while  $\varepsilon > 0$  and  $\mu < 0$  are the coefficients for cubic gain and quintic losses, respectively. Linear losses are accounted for a negative  $\delta$ .

In contrast to the conservative discrete nonlinear Schrödinger (DNLS) equation, the optical power, defined as

$$Q(z) = \sum_{m,n=-M,-N}^{M,N} \psi_{m,n}(z)\psi_{m,n}^*(z) \quad (2)$$

is not a conserved quantity in the present model. However, for a self-localized solution, the power and its evolution will be the main quantity that we will monitor in order to identify different families of stationary and stable solutions.

We look for stationary solutions of Eq.(1) of the form  $\psi_{m,n}(z) = \phi_{m,n} \exp(i\lambda z)$  where  $\phi_{m,n}$  are complex numbers and  $\lambda$  is real; also we are interested in that the phase of solutions changes azimuthally an integer number ( $S$ ) of  $2\pi$  in a closed-circuit. In such a case, the self-localized solution is called a discrete vortex soliton [19] with vorticity  $S$ . By inserting the previous *ansatz* into model (1) we obtain the following set of  $(2M + 1) \times (2N + 1)$  algebraic coupled complex equations:

$$-\lambda\phi_{m,n} + \hat{C}\phi_{m,n} + |\phi_{m,n}|^2\phi_{m,n} + \nu|\phi_{m,n}|^4\phi_{m,n} = i\delta\phi_{m,n} + i\varepsilon|\phi_{m,n}|^2\phi_{m,n} + i\mu|\phi_{m,n}|^4\phi_{m,n}. \quad (3)$$

We have solved equations (3) using a multi-dimensional Newton-Raphson iterative algorithm. The method requires an initial guess, and we have found that usually converges rapidly by starting with a high-localized profile seed that can be constructed by a procedure similar to the one described in [18].

### B. Linear stability analysis

Small perturbations around the stationary solution can grow exponentially, leading to the destruction of the vortex soliton. A linear stability analysis provides us the means for establishing which solutions are stable. Let us to introduce a small perturbation,  $\tilde{\phi}$ , to the localized stationary solution

$$\psi_{m,n} = [\phi_{m,n} + \tilde{\phi}_{m,n}(z)]e^{i\lambda z}, \quad \tilde{\phi}_{m,n} \in \mathbb{C}, \quad (4)$$

then, after replacing Eq.(4) into Eq.(1) and after linearizing with respect to  $\tilde{\phi}$ , we obtain:

$$\begin{aligned} \dot{\tilde{\phi}}_{m,n} + \hat{C}\tilde{\phi}_{m,n} - i\delta\tilde{\phi}_{m,n} + \\ [2(1 - \varepsilon)|\phi_{m,n}|^2 + 3(\nu - \mu)|\phi_{m,n}|^4 - \lambda]\tilde{\phi}_{m,n} + \\ [(1 - \varepsilon)\phi_{m,n}^2 + 2(\nu - \mu)|\phi_{m,n}|^2\phi_{m,n}^2]\tilde{\phi}_{m,n}^* = 0. \end{aligned} \quad (5)$$

The solutions for the above homogeneous linear system can be written as

$$\tilde{\phi}_{m,n}(z) = C_{m,n}^1 \exp[\gamma_{m,n}z] + C_{m,n}^2 \exp[\gamma_{m,n}^*z], \quad (6)$$

being  $C^{1,2}$  integration constants and  $\gamma_{m,n}$  the discrete spectrum of the *eigensystem* associated with (5). The solutions are unstable if at least one eigenvalue has positive real part, that is, if  $\max\{\text{Re}(\gamma_{m,n})\} > 0$ . Hereafter, we will plot stable (unstable) solutions using solid (dashed) lines.

## III. SYMMETRIC AND ASYMMETRIC SOLUTIONS

Eq.(1) has a five-dimensional parameter space, namely  $C, \delta, \varepsilon, \mu, \nu$ . In order to look for any stationary solution, first, we need to choose a fixed set of values for these parameters, and then an initial condition. By starting from a guess with eight peaks surrounding the central site - the first discrete contour of the lattice around of  $(m, n) = (0, 0)$  - with a topological charge  $S = 3$  sampled on this path, the iterative algorithm rapidly converges to a stationary structure with the same features of the initial guess. Once we found a stationary solution with the desired properties, we use it as initial condition to find the corresponding solution for a slightly different set of equation parameters. We usually just change one of them. Therefore, for the dissipative case we construct

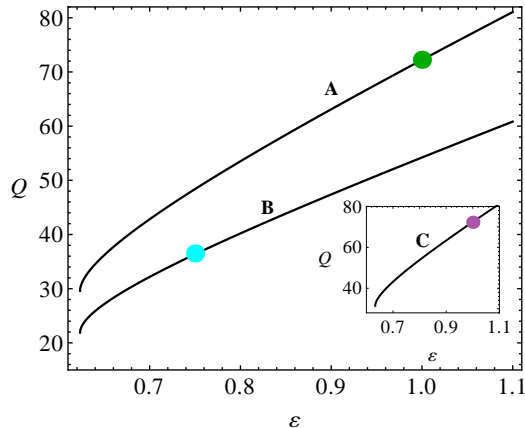


Figure 1. (Color online)  $Q$  versus  $\varepsilon$  diagram for families **A** and **B** of discrete dissipative vortex solitons. Inset:  $Q$  vs.  $\varepsilon$  diagram for family **C**. (CQGL equation parameters:  $C = 0.8$ ,  $\delta = -0.9$ ,  $\mu = -0.1$ ,  $\nu = 0.1$ ).

families of solutions by fixing four parameters and varying the fifth one, usually the cubic gain parameter,  $\varepsilon$ . Using this procedure, we have constructed the **A** family (displayed as the curve  $Q$  versus  $\varepsilon$  in Fig.1). We started from a highly localized solution and we slowly decreased the nonlinear gain, observing that the solution became gradually more and more extended as  $\varepsilon$  (and  $Q$ ) decreased. The saddle-node point for this family is reached at  $\varepsilon \approx 0.62$ .

Fig.2 shows the amplitude and phase profiles corresponding to the solution marked with a green solid circle on the **A** family in Fig.1). From the amplitude profile, Fig.2(a), we can see how the stationary solution maintains the eight excited peaks of the initial seed. Besides, we can see some energy in the tails, i.e. on the second discrete contour. On the other hand, the phase profile, Fig.2(b), clearly shows a topological charge  $S = 3$ .

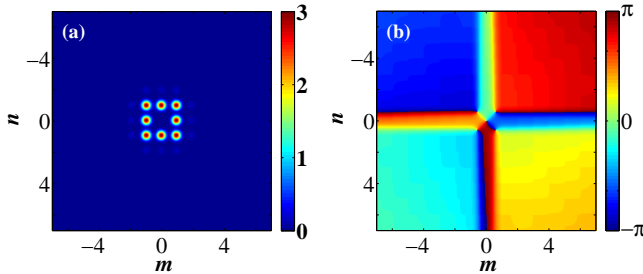


Figure 2. (Color online) Color map plots for the eight peaks stable vortex solution with  $S = 3$ , marked with a green circle on the **A** family branch in Fig.1. (a) Amplitude profile. (b) Phase profile.

A similar procedure has been done to construct another family, labeled **B** (See Fig.1). This family consists of asymmetric stationary solutions characterized for having six peaks displayed on the corners of an elongated hexagon in the  $n$ -axis direction of the lattice. This spa-

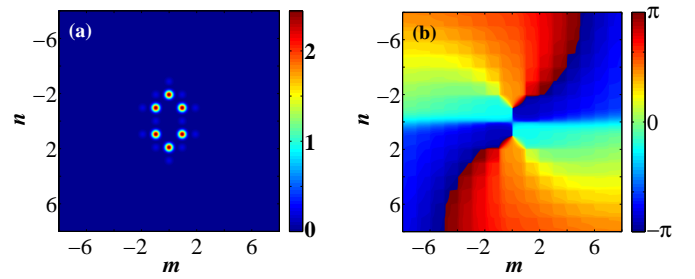


Figure 3. (Color online) Color map plots for the six peaks stable vortex solution with  $S = 2$  marked with a cyan circle on the **A** family branch in Fig.1. (a) Amplitude profile. (b) Phase profile.

tial configuration possesses a topological charge  $S = 2$ . Typical amplitude and phase profiles for this kind of solution are shown as color maps in Fig.3. In the conservative case, four peaks structures have been reported to be stable [19] for  $S = 1$  and unstable for  $S = 2$ ; on the other hand, for hexagonal lattices, six peak structures are stable [20] for  $S = 2$  and unstable for  $S = 1$ . In continuous systems assymetric four peaks structures has been found stable for  $S = 1$  [21].

The families **A** and **B** of stationary vortex solutions coexist for the same set of parameters of the discrete Ginzburg-Landau equation. Other families of solutions exist too for the same set of parameters. The inset shows a different family (the **C**-one), whose  $Q$  vs  $\varepsilon$  diagram almost coincides with the **A**-family one, in spite of being quite different type of solutions. We will describe these **C**-solutions later in Section V.

#### IV. “TWO CHARGES” VORTEX SOLITON

Now, we show one example where two topological charges coexist in the same solution. Let us start with a guess solution consisting of twenty peaks, spatially distributed like a rhombus, and with a topological charge  $S = 2$ . Using it as the starting point for the Newton-Raphson algorithm, we find a stationary solution that looks like the one shown in Fig.4(a,b). This solution belongs to the family displayed in Fig.5 labeled with **D**; it was constructed following the same procedure described in the previous section. Unlike the previous families, the **D** family does not reach the saddle node point *via* a monotonic decreasing of its power; rather, it passes through a minimum value ( $\varepsilon \approx 0.64$ ), then, the power grows and finally, the saddle node point is reached (See inset in Fig.5).

The solutions of this family present a very interesting property related to its topological charge. The first square contour,  $\Gamma_1$ , -the innermost discrete square trajectory on the plane  $(m, n)$ - in Fig.4(b) shows that the vorticity has a value  $S = 2$ . For the second contour  $\Gamma_2$  we observe that the topological charge has changed to

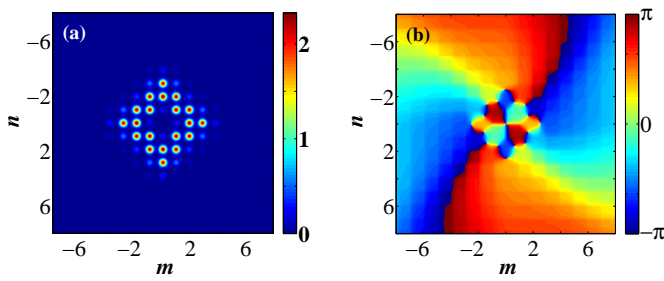


Figure 4. (Color online) Color map plots for the twenty peaks stable two charges ( $S = 2$  and  $S = 6$ ) vortex solution, marked with a green circle on the **D** family in Fig.5. (a) Amplitude profile. (b) Phase profile.

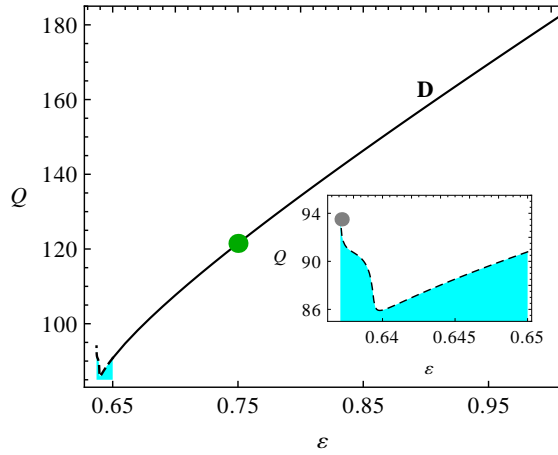


Figure 5. (Color online)  $Q$  versus  $\varepsilon$  diagram for “two charges” ( $S = 2$  and  $S = 6$ ) discrete vortex solitons. Continuous and dashed lines correspond to stable and unstable solutions, respectively. The green circle on the **D** family corresponds to the profiles shown in Fig.4.

$S = 6$ . Looking at the remaining contours, we note that the topological charge returns to  $S = 2$ , so, we can talk about a transition of the effective vorticity from  $S = 2 \rightarrow S = 6 \rightarrow S = 2$ , as we move farther from the center. For this reason, we can say that the stable solutions of this family possess two topological charges. For the sake of clarity, we plot  $\sin(\theta_{m,n})$  vs  $\varphi$ , the azimuthal angle for the lattice, for the first and second discrete contours. From Fig.6(a) we can see that the data (green points) are perfectly fitted by the sinusoidal function (gray line) with two periods ( $S = 2$ ) along the first contour, and for the second contour we have six periods ( $S = 6$ ) as shown in Fig.6(b). This is somehow a proof of the different topological charges contained in the solution, and it also proves that the discrete vortex is a well defined structure.

Fig.5 also shows that the **D** family has one large stable region and another small region, magnified in the inset, where the solutions are unstable. These unstable structures decay on propagation to another kind of stable solutions having less energy, and different amplitude pro-

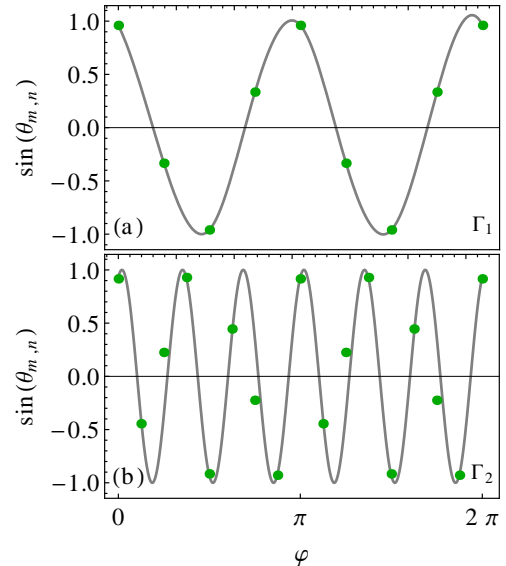


Figure 6. (Color online)  $\sin(\theta_{m,n})$  versus  $\varphi$  (azimuthal angle for the lattice) diagram for the first (a) and second (b) discrete contour for the vortex soliton, marked with a green dot on the **D** family in Fig.5

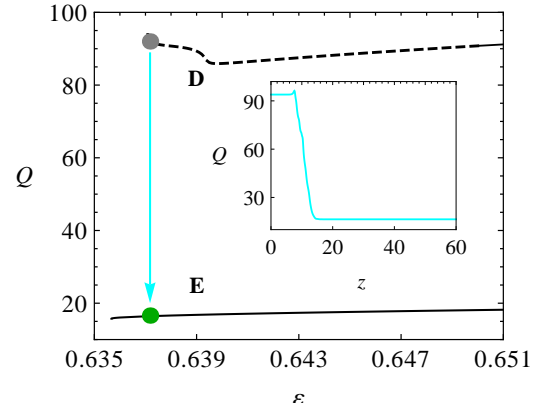


Figure 7. (Color online)  $Q$  versus  $\varepsilon$  diagram showing the transition from the unstable solution marked with the gray circle to the stable solution marked with the green circle; the inset shows the power evolution for this transition.

file with only four peaks. In particular, Fig.7 illustrates how the unstable solution marked with a gray point (the saddle-node point for the **D** family in the Fig.4) decays, by means of a radiative process shown in the inset, to the stable solution marked with a green circle on the **E** family. The amplitude and phase profiles showed in Figs.8(a-b) and Figs.8(c-d) correspond to the unstable and stable solutions marked with gray and green circles in Fig.7.

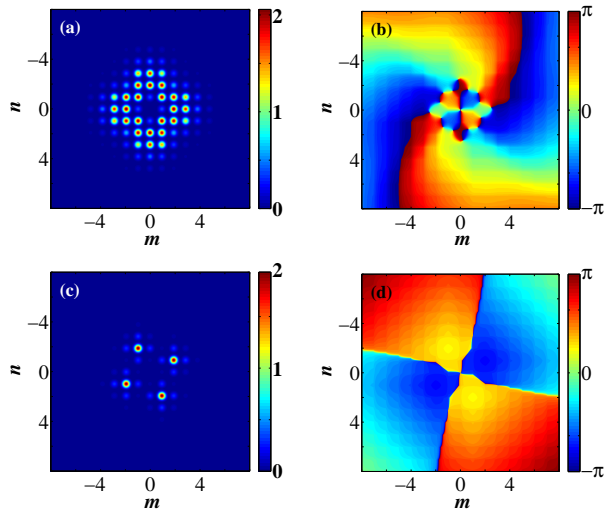


Figure 8. (Color online) Color map plots for discrete dissipative solitons. (a) Amplitude profile and (b) phase profile for the unstable twenty peaks vortex solution localized on the **D** family at the gray circle in the Fig.7. (c) Amplitude profile and (d) phase profile for the four peaks soliton solution localized on the **E** family at the green circle in the Fig.7

## V. DISSIPATION AND STABILITY

In this section, we are interested in analyzing how the stability of the solutions is affected when our model slowly goes to the Schrödinger limit, i.e when the value of the parameters in the CQGL equation (1) tends to zero:  $\{\delta, \epsilon, \mu, \nu\} \rightarrow 0$ . In particular we will focus on the solution marked with a purple circle on the **C** family in the inset of Fig.1. We will compute its stability region when the gain, loss and higher order Kerr terms are gradually suppressed in the Ginzburg-Landau model.

These solutions are of the “two-charges” vortex type, with charges  $S = 1$  and  $S = -3$  [18]. Moreover, this type of solutions (the swirl-vortex soliton) can be understood as a bound state of five vortices [22, 23]. Indeed, we can identify a vortex with  $S = 1$  at the origin ( $\circlearrowright$  symbol), surrounded by four vortex, each with  $S = -1$ , whose singularities are located at the center of the  $\circlearrowleft$  symbols on the Fig.9(b). This interpretation agrees with the transition of the effective vorticity from  $S = 1 \rightarrow S = -3$ , as we move farther from the center. The amplitude and phase profiles for this solution are displayed in Fig.9(a-b). It should be noted that it has the same power value that the solution marked with the green circle on the **A** family. (In fact, we plot its corresponding family in the inset because both families have almost identical  $Q$  versus  $\varepsilon$  diagrams). We can see that both amplitude profiles are very different; even though each one has eight principal excited sites, their spatial distributions are dissimilar. In addition, their phase profiles are completely different. While the solutions on the **A** family have a well defined unique topological charge  $S = 3$ , the solutions on the **C**

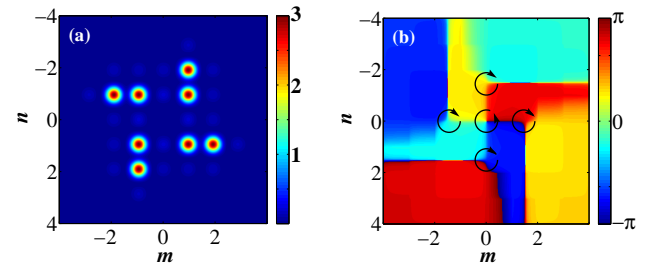


Figure 9. (Color online) Color map plots for the eight peaks stable two charges ( $S = 1$  and  $S = -3$ ) vortex solution localized on the **C** family at the purple circle in the Fig.1. (a) Amplitude profile. (b) Phase profile.

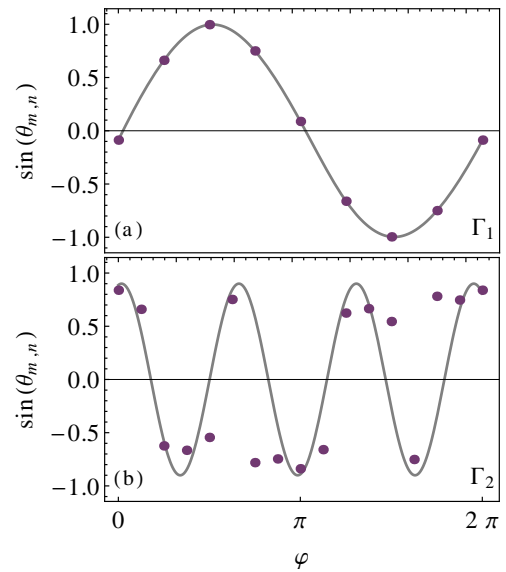


Figure 10. (Color online)  $\sin(\theta_{m,n})$  versus  $\varphi$  (azimuthal angle) for the lattice diagram for the first (a) and second (b) discrete contour for the swirl-vortex soliton, marked with a purple dot on the **C** family in Fig.1.

family have two charges ( $S = 1$  and  $S = -3$ ) simultaneously, as mentioned before. Again, we plot  $\sin(\theta_{m,n})$  vs  $\varphi$  for the first ( $\Gamma_1$ ) and the second ( $\Gamma_2$ ) discrete contour. From Fig.10(a) we can see one period ( $S = 1$ ) for the sinusoidal function (gray line) along the first contour, and for the second contour we have three periods ( $S = -3$ ) as shown in Fig.10(b). Unlike the conservative cubic case (NLSE), in the dissipative model the propagation constant  $\lambda$  is not an arbitrary parameter that can be chosen at will. It is fixed by the rest of the CQGL equation parameters. By changing them, the value of the propagation constant also changes. As in other nonlinear problems [24], we can think of the dissipative terms as determinant to select one of the infinite solutions of the associated conservative problem. With this in mind we will find out the stability regions in terms of the propagation constant so we can compare with the Schrödinger limit.

For the sake of comparison we construct the  $Q$  versus  $\lambda$  diagram shown in Fig.11. Here, we have fixed  $\delta$ ,  $\mu$  and  $\nu$  parameters and we only move through the  $\varepsilon$  parameter (nonlinear gain). In this way, we obtain a solution and its corresponding propagation constant for each value of  $\varepsilon$ . Then, we proceed varying the rest of the parameters slightly, and construct a new curve, taking the solutions of the previous curve as initial conditions in our multidimensional Newton-Raphson scheme. In the inset of Fig.11 we show the corresponding  $\lambda$  vs  $\varepsilon$  diagram.

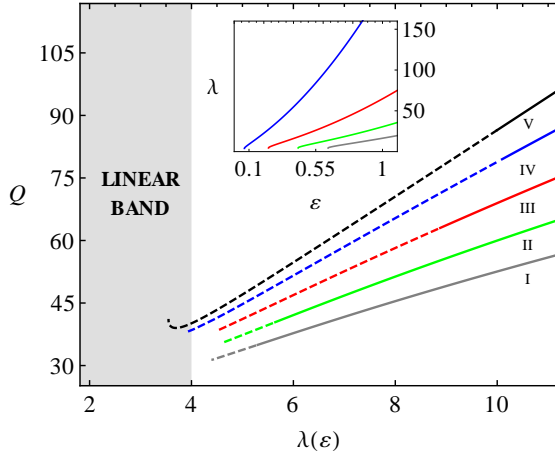


Figure 11. (Color online)  $Q$  versus  $\lambda(\varepsilon)$  diagram for several sets of parameters specified in Table I, of two charges swirl-vortex solitons. Inset shows  $\lambda$  vs  $\varepsilon$ .

With the previous scheme we can find a large number of curves, but for the sake of clarity, we only show three of them; they are located between the conservative cubic case (black branch) and the **C** curve (gray branch). We can read from Table I the CQGL equation parameters corresponding to the curves displayed in Fig.11. These five branches belong to the same family conformed by vortex solutions with amplitude and phase profiles such as those showed in Fig.9.

We have done the standard linear stability analysis, described in section II, for each one of them. The part of the curves that correspond to stable solutions are shown with continuous lines while the dashed lines correspond to unstable solutions.

Taking the above into account, we can clearly establish that if the dissipation is attenuated the stability regions for the soliton solutions are reduced. [24] Indeed, we can see here a wide difference between the stability regions for the Schrödinger limit and the **C** branch. The first one only has stable solutions for propagation constant values far away from the linear band, the last one has stable solutions for propagation constant values closer to the linear band.

Table I. CQGL equation parameters

Curve	$\delta$	$\mu$	$\nu$
I	-0.9	-0.1	0.1
II	-0.8	-0.08	0.08
III	-0.4	-0.03	0.03
IV	-0.1	-0.01	0.01
V	0	0	0

## VI. SUMMARY AND CONCLUSIONS

In conclusion, we have found discrete vortex solitons (symmetric and asymmetric) with higher-order vorticity in dissipative 2D-lattices and studied its stability. In particular, we have also shown in detail a solution that contains two topological charges. Finally, we analyzed the stability of the solutions when dissipation in the system is decreased, observing that the stability regions shrink. A comparison with the conservative cubic case is done, showing that dissipation serves to provide stability to otherwise unstable conservative solutions.

## VII. ACKNOWLEDGMENTS

C.M.C. and J.M.S.C. acknowledge support from the Ministerio de Ciencia e Innovación under contracts FIS2006-03376 and FIS2009-09895. R.A.V and M.I.M acknowledge support from FONDECYT, Grants 1080374 and 1070897, and from Programa de Financiamiento Basal de CONICYT (FB0824/2008).

---

[1] C. López-Mariscal and Julio C. Gutiérrez-Vega. In your phase: All about optical vortices. *Optics and Photonics News*, 82(6):10–14, May 2009.

[2] Anton S. Desyatnikov, Yuri S. Kivshar, and Lluis Torner. Optical vortices and vortex solitons. volume 47 of *Progress in Optics*, pages 291 – 391. Elsevier, 2005.

[3] David K. Campbell, Sergej Flach, and Yuri S. Kivshar. Localizing energy through nonlinearity and discreteness. *Physics Today*, 57(1):43–49, 2004.

[4] Falk Lederer, George I. Stegeman, Demetri N. Christodoulides, Gaetano Assanto, Moti Segev, and Yaron Silberberg. Discrete solitons in optics. *Physics Reports*, 463(1-3):1 – 126, 2008.

[5] Sergej Flach and Andrey V. Gorbach. Discrete breathers – advances in theory and applications. *Physics Reports*, 467(1-3):1 – 116, 2008.

[6] Rodrigo A. Vicencio, Mario I. Molina, and Yuri S. Kivshar. Controlled switching of discrete solitons in waveguide arrays. *Opt. Lett.*, 28(20):1942–1944, Oct 2003.

[7] N. Akhmediev and A. Ankiewicz. *Dissipative Solitons. Lecture Notes in Physics*, Vol. 661 (Springer, Berlin,

2005). Springer, New York, 2005.

[8] J. M. Soto-Crespo, N. Akhmediev, and G. Town. Interrelation between various branches of stable solitons in dissipative systems—conjecture for stability criterion. *Optics Communications*, 199(1-4):283 – 293, 2001.

[9] N. Akhmediev and A. Ankiewicz. *Dissipative Solitons: From optics to biology and medicine. Lecture Notes in Physics, Vol. 751 (Springer, Berlin, 2008)*. Springer, New York, 2008.

[10] H. S. Eisenberg, Y. Silberberg, R. Morandotti, A. R. Boyd, and J. S. Aitchison. Discrete spatial optical solitons in waveguide arrays. *Phys. Rev. Lett.*, 81(16):3383–3386, Oct 1998.

[11] Jason W. Fleischer, Mordechai Segev, Nikolaos K. Efremidis, and Demetrios N. Christodoulides. Observation of two-dimensional discrete solitons in optically induced nonlinear photonic lattices. *Nature*, 422(16):147–150, Mar 2003.

[12] B. A. Malomed and P. G. Kevrekidis. Discrete vortex solitons. *Phys. Rev. E*, 64(2):026601, Jul 2001.

[13] Dragomir N. Neshev, Tristram J. Alexander, Elena A. Ostrovskaya, Yuri S. Kivshar, Hector Martin, Igor Makasyuk, and Zhigang Chen. Observation of discrete vortex solitons in optically induced photonic lattices. *Phys. Rev. Lett.*, 92(12):123903, Mar 2004.

[14] Edward Arévalo. Soliton theory of two-dimensional lattices: The discrete nonlinear schrödinger equation. *Phys. Rev. Lett.*, 102(22):224102, Jun 2009.

[15] J. M. Soto-Crespo, N. Akhmediev, C. Mejía-Cortés, and N. Devine. Dissipative ring solitons with vorticity. *Opt. Express*, 17(6):4236–4250, Mar 2009.

[16] V. Skarka, N. B. Aleksic, H. Leblond, B. A. Malomed, and D. Mihalache. Varieties of stable vortical solitons in ginzburg-landau media with radially inhomogeneous losses. *Phys. Rev. Lett.*, 105(21):213901, Nov 2010.

[17] Hervé Leblond, Boris A. Malomed, and Dumitru Mihalache. Stable vortex solitons in the ginzburg-landau model of a two-dimensional lasing medium with a transverse grating. *Phys. Rev. A*, 80(3):033835, Sep 2009.

[18] C. Mejía-Cortés, J. M. Soto-Crespo, Mario I. Molina, and Rodrigo A. Vicencio. Dissipative vortex solitons in two-dimensional lattices. *Phys. Rev. A*, 82(6):063818, Dec 2010.

[19] D.E. Pelinovsky, P.G. Kevrekidis, and D.J. Frantzeskakis. Persistence and stability of discrete vortices in nonlinear schrödinger lattices. *Physica D: Nonlinear Phenomena*, 212(1-2):20 – 53, 2005.

[20] Bernd Terhalte, Tobias Richter, Kody J. H. Law, Dennis Göries, Patrick Rose, Tristram J. Alexander, Panayotis G. Kevrekidis, Anton S. Desyatnikov, Wieslaw Krolikowski, Friedemann Kaiser, Cornelia Denz, and Yuri S. Kivshar. Observation of double-charge discrete vortex solitons in hexagonal photonic lattices. *Phys. Rev. A*, 79(4):043821, Apr 2009.

[21] Tristram J. Alexander, Andrey A. Sukhorukov, and Yuri S. Kivshar. Asymmetric vortex solitons in nonlinear periodic lattices. *Phys. Rev. Lett.*, 93(6):063901, Aug 2004.

[22] Miguel-Ángel García-March, Albert Ferrando, Mario Zacarés, Sarira Sahu, and Daniel E. Ceballos-Herrera. Symmetry, winding number, and topological charge of vortex solitons in discrete-symmetry media. *Phys. Rev. A*, 79(5):053820, May 2009.

[23] C. Chong, R. Carretero-González, B.A. Malomed, and P.G. Kevrekidis. Multistable solitons in higher-dimensional cubic-quintic nonlinear schrödinger lattices. *Physica D: Nonlinear Phenomena*, 238(2):126 – 136, 2009.

[24] J. M. Soto-Crespo, N. N. Akhmediev, B. C. Collings, S. T. Cundiff, K. Bergman, and W. H. Knox. Polarization-locked temporal vector solitons in a fiber laser: theory. *J. Opt. Soc. Am. B*, 17(3):366–372, Mar 2000.

